Article

One-Pot Synthesis of Epirubicin-Capped Silver Nanoparticles and Their Anticancer Activity against Hep G2 Cells

Jun Ding [1,2] , **Guilin Chen [1,3]** , **Guofang Chen [4,*]** and **Mingquan Guo [1,3,*]**

[1] Key Laboratory of Plant Germplasm Enhancement & Specialty Agriculture, Wuhan Botanical Garden, Chinese Academy of Sciences, Wuhan 430074, China; sophia_dj@126.com (J.D.); glchen@wbgcas.cn (G.C.)
[2] Key Laboratory of Analytical Chemistry for Biology and Medicine (Ministry of Education), Department of Chemistry, Wuhan University, Wuhan 430072, China
[3] Sino-Africa Joint Research Center, Chinese Academy of Sciences, Wuhan 430074, China
[4] Chemistry Department, St. John's University, Queens, New York, NY 11439, USA
[*] Correspondence: gfchen08@yahoo.com or cheng@stjohns.edu (G.C.); guomq@wbgcas.cn (M.G.); Tel.: +86-27-8770-0850 (M.G.)

check for updates

Abstract: Epirubicin-capped silver nanoparticles (NPs) were synthesized through a one-pot method by using epirubicin as both the functional drug and the reducing agent of Ag^+ to Ag^0. The preparation process was accomplished in 1 h. In addition, the obtained epirubicin-capped silver nanoparticle was characterized by transmission electron microscopy (TEM), energy-dispersive X-ray spectroscopy (EDX), and infrared spectroscopy. The results showed that a layer of polymer epirubicin had formed around the silver nanoparticle, which was 30-40 nm in diameter. We further investigated the antitumor activity of the prepared epirubicin-capped silver nanoparticle, and the half maximal inhibitory concentration (IC_{50}) against Hep G2 cells was 1.92 µg/mL, indicating a good antitumor property of the nanoparticle at low dosage.

Keywords: epirubicin; one-pot synthesis; silver nanoparticle; antitumor

1. Introduction

Nanoparticles (NPs), ranging from 1 to 100 nm in size, have gained considerable interest because of their various potential applications in clinical nanomedicine and research [1–3]. Noble metal NPs, especially silver NPs, with the properties of large specific surface area, enhanced surface plasmon resonance, and minimal side effects have been proposed for potential use in the anticancer area [4,5]. For instance, Ag NPs of approximately 50 nm in size can target tumor tissues based on the enhanced permeation and retention (EPR) effect [6,7], and the photo-thermal conversion in Ag NPs can increase the temperature locally, thereby achieving therapeutic killing of tumor cells [8–10]. Clearly, Ag NPs represent a promising anticancer agent with the assistance of photo-thermal therapy. However, the therapeutic effect of bare Ag NPs is limited. The functionalization of Ag NPs with anticancer drugs is a promising method to provide synergistic effects by combining both therapeutic actions, resulting in better anticancer effects.

Typically, drug-loaded Ag NPs are fabricated by top-down and bottom-up approaches. In the top-down method, a silver NP core is first obtained, and then post-modification and drug-loading steps are performed [11,12]. Obviously, the process is complicated and time-consuming, and the morphology control of the final particles is also troublesome. As for bottom-up methods, drugs could be incorporated directly into Ag NPs during the growth of starting materials, which is more convenient. However, the chemical reducing agent required by the method, such as $NaBH_4$, pyridine, etc.,

might lead to the presence of toxic reagents existing on or in Ag NPs [13], which would bring about adverse effects in further biological or medical applications. Moreover, the recently reported bottom-up methods mostly chose to load plant extract onto Ag NPs [14–16], possibly resulting in an undefined curative effect or side effect. Therefore, a new green and simple strategy to prepare drug-capped Ag NPs is highly favorable.

Epirubicin (Figure 1) is an anticancer prescription medicine for chemotherapy [17], which is proved to be effective to treat breast, lung, and liver cancers. It possesses several phenolic hydroxyl groups, thus exhibiting a weak reduction property. In this study, we employed epirubicin as the functional drug and also the reducing agent, thereby developing a novel, green, and mild method to synthesize epirubicin-capped silver NPs by the chemical reaction process between the silver salt solution and epirubicin without using any surfactant. Subsequently, the antitumor effect of the resultant NPs was evaluated.
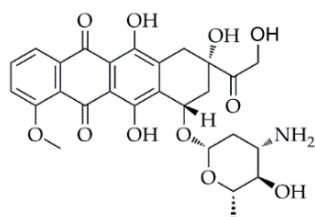

Figure 1. Structure of epirubicin.

2. Materials and Methods

2.1. Chemicals and Reagents

Silver nitrate (99.8%) was obtained from Aladdin (Shanghai, China). Epirubicin (98%) was purchased from Melonepharma (Dalian, China). Fetal calf serum (FCS) was purchased from Sijiqing Co. (Hangzhou, China). Dulbecco's modified eagle medium was supplied by Gibco (Waltham, MA, USA). 3-(4,5-Dimethylthiazol-2-yl)-2,5-diphenyltetrazolium bromide (MTT) was obtained from Biosharp (Hefei, China). Ultra-pure water used throughout the study was purified with the Milli-Q system (Millipore, Bedford, MA, USA).

2.2. Preparation of Epirubicin-Capped Silver NPs

Epirubicin-capped silver NPs were obtained using a green and mild procedure [18,19]. First, a $AgNO_3$-MilliQ water solution (10^{-2} M) was heated till boiling at 120 °C under magnetic stirring. Subsequently, an epirubicin solution was added to obtain the final concentration of 10^{-4} (w/v). After reacting at 120 °C for 1 h, the resultant epirubicin-capped silver NPs were obtained. Subsequently, excess unreacted epirubicin was removed by dialysis in ultra-pure water for 48 h [20,21]. The final product was obtained by centrifugation at $10,000 \times g$ for 30 min.

2.3. Characterization of Epirubicin-Capped Silver NPs

TEM images were obtained using JEM-100CXII transmission electron 135 microscopes (TEM, Jeol, Tokyo, Japan). FT-IR spectra were obtained using an AVATAR 137 360 FT-IR spectrometer (Thermo Electron Inc., San Jose, CA, USA). The chemical composition of epirubicin-capped silver NPs was examined by EDX-720 energy-dispersive X-ray analysis (EDX, Shimadzu, Kyoto, Japan) using Mg Kα radiation as the excitation source.

2.4. Cytotoxicity Assay

The cytotoxic effect of the epirubicin silver NPs at various concentrations against Hep G2 cells was evaluated by the MTT assay [22], and the absorbance in MTT assay was measured by a BioTek EL-x800 microplate reader (Bio-Tek Instruments Inc, Winooski, VT, USA). In brief, approximately

30,000 Hep G2 cells were seeded in a 96-well flat-bottom tissue culture plate. After cultivation for 24 h, they were exposed to the NPs at concentrations ranging from 0 to 30 µg/mL, and epirubicin at concentrations in the range of 0–50 µg/mL, respectively for 48 h. After treatment, the supernatant was removed and washed with phosphate-buffered saline (PBS), and then a 20 µL portion of MTT reagent (5 mg/mL) was added to each well and incubated overnight at 37 °C for 4 h to permit the formation of purple formazan crystals. Subsequently, the supernatant was discarded, and a 150 µL portion of DMSO was added in the well to dissolve the purple formazan crystals. Finally, the absorbance was measured at 570 nm using a microplate reader. The inhibition rate was calculated by subtracting the absorbance of samples treated with silver NPs or epirubicin from that of the negative controls, and then comparing it to the absorbance of the negative controls.

3. Results and Discussion

3.1. Characterization

The morphology of the as-synthesized NPs was investigated by transmission electron microscopy (TEM). The TEM image (Figure 2) shows that the NPs exhibit spherical and uniform morphologies with an average diameter of 36 mm, and a layer of film is observed to cap around the NPs, which was believed to be a layer of poly-epirubicin and epirubicin complex formed during the Ag^+ reduction process. The resultant Ag NPs are of a suitable size to be retained among the tumor tissues, which makes them a good passive targeting agent.
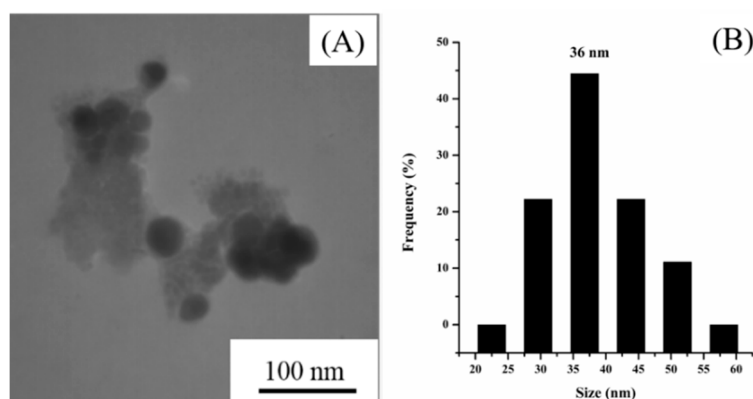

Figure 2. (**A**) Image and (**B**) size distribution diagram of epirubicin-capped silver nanoparticles (NPs).

To further demonstrate the successful preparation of epirubicin-capped silver NPs, the composition was examined by energy-dispersive X-ray spectroscopy (EDX). As shown in Figure 3, the NPs were clearly constituted by Ag, C, and O. The existence of C and O indicates organic compounds were incorporated into the obtained NPs, which is ascribed to poly-epirubicin or epirubicin.
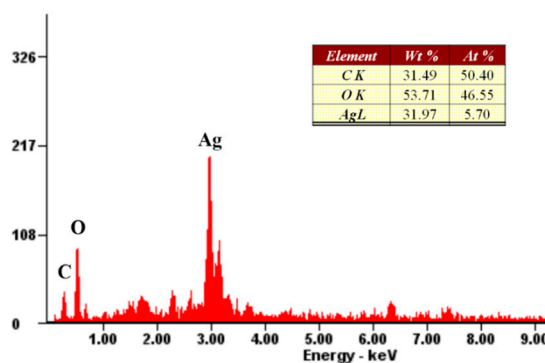

Element	Wt %	At %
C K	31.49	50.40
O K	53.71	46.55
Ag L	31.97	5.70

Figure 3. Energy-dispersive X-ray spectroscopy (EDX) spectrum and chemical composition (the inset table) of epirubicin-capped silver NPs.

Furthermore, infrared spectroscopy was employed to understand the formation mechanism of the epirubicin-capped silver NP. The IR spectra of epirubicin and epirubicin-capped silver NPs were obtained, respectively. Figure 4A shows the IR spectrum of epirubicin. The presence of two peaks at 2920 cm^{-1} and 2850 cm^{-1} is assigned to the stretching vibration of the CH$_2$ group, whereas the presence of the absorption peak at 1385 cm^{-1} belongs to the bending vibration of CH$_2$. The peak at 1632 cm^{-1} is attributed to a contemporaneous contribution of C=C and C=O stretching mode, and the broad peaks at 3435 cm^{-1} correspond to the O–H stretching vibration of water. Specifically, the signal at 1276 cm^{-1} and 1210 cm^{-1} is derived from the ν (C–O) of the enol function. From the IR spectrum of epirubicin-capped silver NPs as shown in Figure 4B, the existing peaks in the range of 3000–1300 cm^{-1} were similar to that of epirubicin, indicating the successful coating of epirubicin onto silver NPs. In particular, the signals at 1276 cm^{-1} and 1210 cm^{-1}, attributable to the C–O stretching mode of the enol, disappeared, which might be ascribed to the oxidation of the phenolic hydroxyl groups into quinone or phenolic ether. It is believed that during the oxidation process of epirubicin, epirubicin acted as a reducing reagent, which converted Ag$^+$ into silver NPs, and in the meantime epirubicin was capped onto the surface of the silver NPs, leading to the successful formation of the resultant epirubicin-capped Ag NPs. It is also worth mentioning that after standing the prepared epirubicin-capped silver NPs in water for 30 days at room temperature, there was no change in morphology or composition observed (data not shown), indicating a good stability of the prepared nanoparticles.
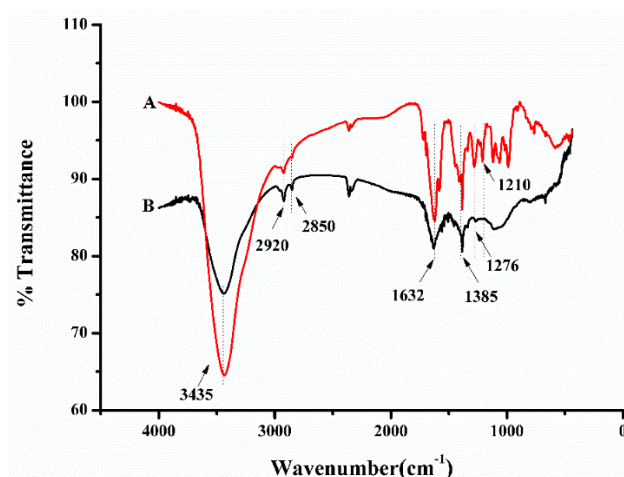

Figure 4. FT-IR spectra of (**A**) epirubicin and (**B**) epirubicin-capped silver NPs.

3.2. Evaluation of Antitumor Activity

To demonstrate the antitumor activity of the obtained epirubicin-capped silver NPs, the cytotoxicity of the Ag NPs was investigated using the 3-(4,5-dimethylthiazol-2-yl)-2,5-diphenyltetrazolium bromide (MTT) method, and Hep G2 cells were chosen as the target cell line. To this end, Hep G2 cells were cultivated with free epirubicin and epirubicin-capped silver NPs in a series of diverse concentrations, respectively. After cultivation for 72 h, the cell viabilities were obtained. Based on this result, the concentrations of IC$_{50}$ for both free epirubicin and epirubicin-capped silver NPs toward Hep G2 cells were calculated from the survival curves. As shown in Figure 5 and Table 1, the IC$_{50}$ values of epirubicin-capped silver NPs and epirubicin were 1.92 μg/mL (hill slope at 2.43) and 0.11 μg/mL (hill slope at 0.57), respectively [23–25], which means that the Ag NPs gave a remarkably increased IC$_{50}$ value compared with free epirubicin, but still fell well within the proper range of most anticancer drug candidates in terms of IC$_{50}$ values. The obtained hill slopes also indicated that epirubicin-capped NPs exhibited positive cooperativity, whereas epirubicin exerted negative cooperativity of binding. The difference in binding behavior between epirubicin-capped silver NPs and free epirubicin could be ascribed to the incorporation of silver NPs with epirubicin. In fact,

when applying free epirubicin directly onto the cancer patient, several side effects and toxicity were observed as a relatively large dose of the drug was taken at one time, leading to a sudden rise and rapid fall of the drug concentration in blood. In the case of using epirubicin silver NPs as the antitumor drug, the silver NPs could target the tumor tissues based on EPR because of the suitable size of the NPs, making the normal tissue free from the drug. Furthermore, epirubicin was wrapped onto the silver NPs in the form of a polymer and it could be slowly released to the tumor tissue, thus significantly lowering the cytotoxicity compared to free epirubicin [26,27]. This result convincingly demonstrates that the as-prepared Ag NPs are promising antitumor agents at low dosage. Moreover, we compared the performance of the prepared epirubicin-capped silver NPs with other epirubicin-loaded systems. According to the data summarized in Table 2, our system exhibits superior cytotoxic activity with lower IC_{50} values [28–30].
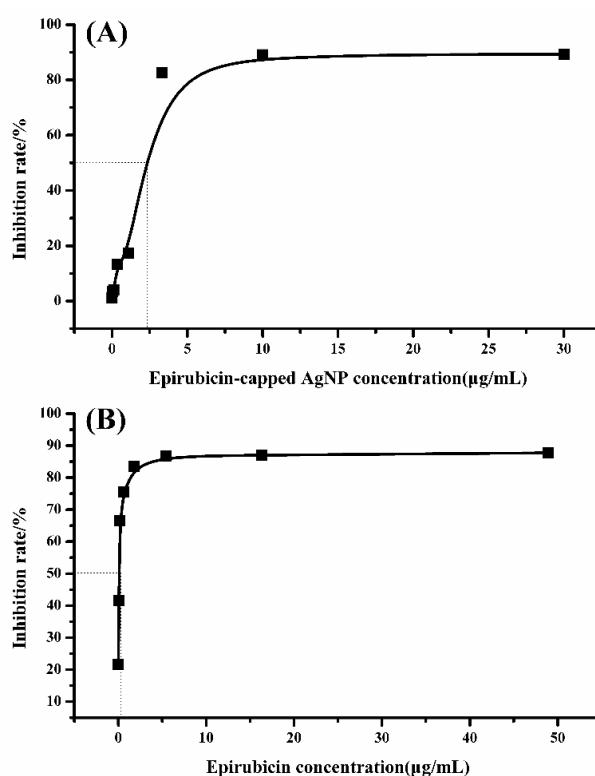

Figure 5. Inhibition curve of (**A**) epirubicin-capped silver NPs and (**B**) epirubicin for the Hep G2 cell line.

Table 1. IC_{50} and hill slopes of epirubicin-capped silver NPs and epirubicin.

Drug	IC50 (µg/mL)	Hill Slope
Epirubicin-capped silver NPs	1.92	2.43
Epirubicin	0.11	0.57

Table 2. Comparison of cytotoxic activities of reported epirubicin drug systems.

Nanoparticle	Cell	IC_{50}	Reference
Epirubicin-loaded folate-modified PA nanoparticles	Human nasopharyngeal epidermal carcinoma cell	2.75 µg/mL	[28]
Epirubicin-loaded PLGA/TPGS nanoparticles	Hep G2 cells	0.78 µg/mL	[29]
Epirubicin-loaded poly(lactic-*co*-glycolic acid) nanoparticles	MCF-7 cells	824 nM	[30]
Epirubicin-capped silver NPs	Hep G2 cells	0.11 µg/mL	This work

4. Conclusions

In summary, we have presented a one-pot synthesis method for fabricating epirubicin-capped silver NPs. The reaction was accomplished by the fast chemical reaction between a silver salt solution and epirubicin without using any surfactant, thus making the method simple, green, and mild. The resultant epirubicin-capped silver NPs exhibited a great anticancer property at low dosage. Considering the mechanisms of the synthesis method, the universality of the proposed method should be further evaluated, which is an ongoing study in our laboratory. Taken together, this approach represents a new option for preparing drug-loaded Ag NPs with a broad application prospect in clinic.

Author Contributions: G.C. (Guofang Chen) and M.G. conceived and designed the research, J.D. and G.C. (Guilin Chen) performed the research, analyzed the data, and wrote the paper. All authors reviewed and approved the manuscript.

Conflicts of Interest: The authors declare no competing financial interests. The funders played no role in the study design, data collection and analysis, and decision to publish.

References

1. Burda, C.; Chen, X.B.; Narayanan, R.; El-Sayed, M.A. Chemistry and properties of nanocrystals of different shapes. *Chem. Rev.* **2005**, *105*, 1025–1102. [CrossRef] [PubMed]
2. Rosi, N.L.; Mirkin, C.A. Nanostructures in biodiagnostics. *Chem. Rev.* **2005**, *105*, 1547–1562. [CrossRef] [PubMed]
3. Wang, A.Z.; Langer, R.; Farokhzad, O.C. Nanoparticle delivery of cancer drugs. *Annu. Rev. Med.* **2012**, *6363*, 185–198. [CrossRef] [PubMed]
4. Lok, C.N.; Zou, T.; Zhang, J.J.; Lin, I.W.S.; Che, C.M. Controlled-release systems for metal-based nanomedicine: Encapsulated/self-assembled nanoparticles of anticancer gold(iii)/platinum(ii) complexes and antimicrobial silver nanoparticles. *Adv. Mater.* **2014**, *26*, 5550–5557. [CrossRef] [PubMed]
5. Locatelli, E.; Naddaka, M.; Uboldi, C.; Loudos, G.; Fragogeorgi, E.; Molinari, V.; Pucci, A.; Tsotakos, T.; Psimadas, D.; Ponti, J.; et al. Targeted delivery of silver nanoparticles and alisertib: In vitro and in vivo synergistic effect against glioblastoma. *Nanomedicine* **2014**, *9*, 839–849. [CrossRef]
6. Prabhakar, U.; Maeda, H.; Jain, R.K.; Sevick-Muraca, E.M.; Zamboni, W.; Farokhzad, O.C.; Barry, S.T.; Gabizon, A.; Grodzinski, P.; Blakey, D.C. Challenges and key considerations of the enhanced permeability and retention effect for nanomedicine drug delivery in oncology. *Cancer Res.* **2013**, *73*, 2412–2417. [CrossRef] [PubMed]
7. Duncan, R.; Sat-Klopsch, Y.N.; Burger, A.M.; Bibby, M.C.; Fiebig, H.H.; Sausville, E.A. Validation of tumour models for use in anticancer nanomedicine evaluation: The epr effect and cathepsin b-mediated drug release rate. *Cancer Chemother. Pharmacol.* **2013**, *72*, 417–427. [CrossRef] [PubMed]
8. Boca, S.C.; Potara, M.; Gabudean, A.M.; Juhem, A.; Baldeck, P.L.; Astilean, S. Chitosan-coated triangular silver nanoparticles as a novel class of biocompatible, highly effective photothermal transducers for in vitro cancer cell therapy. *Cancer Lett.* **2011**, *311*, 131–140. [CrossRef] [PubMed]
9. Di Corato, R.; Palumberi, D.; Marotta, R.; Scotto, M.; Carregal-Romero, S.; Rivera, G.P.; Parak, W.J.; Pellegrino, T. Magnetic nanobeads decorated with silver nanoparticles as cytotoxic agents and photothermal probes. *Small* **2012**, *8*, 2731–2742. [CrossRef]
10. Jain, P.K.; Huang, X.H.; El-Sayed, I.H.; El-Sayed, M.A. Noble metals on the nanoscale: Optical and photothermal properties and some applications in imaging, sensing, biology, and medicine. *Acc. Chem. Res.* **2008**, *41*, 1578–1586. [CrossRef] [PubMed]
11. Wu, W.; Zhou, T.; Berliner, A.; Banerjee, P.; Zhou, S. Smart core−shell hybrid nanogels with ag nanoparticle core for cancer cell imaging and gel shell for ph-regulated drug delivery. *Chem. Mater.* **2010**, *22*, 1966–1976. [CrossRef]

12. Zong, S.; Wang, Z.; Yang, J.; Wang, C.; Xu, S.; Cui, Y. A sers and fluorescence dual mode cancer cell targeting probe based on silica coated au@ag core–shell nanorods. *Talanta* **2012**, *97*, 368–375. [CrossRef]

13. Shenashen, M.A.; El-Safty, S.A.; Elshehy, E.A. Synthesis, morphological control, and properties of silver nanoparticles in potential applications. *Part. Part. Syst. Charact.* **2014**, *31*, 293–316.

14. Begum, N.A.; Mondal, S.; Basu, S.; Laskar, R.A.; Mandal, D. Biogenic synthesis of au and ag nanoparticles using aqueous solutions of black tea leaf extracts. *Colloid. Surf. B* **2009**, *71*, 113–118.

15. Krishnaraj, C.; Jagan, E.G.; Rajasekar, S.; Selvakumar, P.; Kalaichelvan, P.T.; Mohan, N. Synthesis of silver nanoparticles using acalypha indica leaf extracts and its antibacterial activity against water borne pathogens. *Colloid. Surf. B* **2010**, *76*, 50–56. [CrossRef] [PubMed]

16. Mittal, A.K.; Bhaumik, J.; Kumar, S.; Banerjee, U.C. Biosynthesis of silver nanoparticles: Elucidation of prospective mechanism and therapeutic potential. *J. Colloid Interface Sci.* **2014**, *415*, 39–47. [CrossRef] [PubMed]

17. Nagata, M.; Matsuo, Y.; Hidaka, M.; Kawano, Y.; Okumura, M.; Tokunaga, J.; Takamura, N.; Arimori, K. Effect of acute hepatic failure on epirubicin pharmacokinetics after intrahepatic arterial injection in rats. *Biol. Pharm. Bull.* **2008**, *31*, 493–496. [CrossRef]

18. Li, S.Y.; Wang, M. Novel core–shell structured paclitaxel-loaded plga@ag–au nanoparticles. *Mater. Lett.* **2013**, *92*, 350–353. [CrossRef]

19. Bettini, S.; Pagano, R.; Valli, L.; Giancane, G. Drastic nickel ion removal from aqueous solution by curcumin-capped ag nanoparticles. *Nanoscale* **2014**, *6*, 10113–10117. [PubMed]

20. Sweeney, S.F.; Woehrle, G.H.; Hutchison, J.E. Rapid purification and size separation of gold nanoparticles via diafiltration. *J. Am. Chem. Soc.* **2006**, *128*, 3190–3197. [CrossRef] [PubMed]

21. Min, K.H.; Park, K.; Kim, Y.S.; Bae, S.M.; Lee, S.; Jo, H.G.; Park, R.W.; Kim, I.S.; Jeong, S.Y.; Kim, K.; et al. Hydrophobically modified glycol chitosan nanoparticles-encapsulated camptothecin enhance the drug stability and tumor targeting in cancer therapy. *J. Control. Release* **2008**, *127*, 208–218. [CrossRef]

22. Skehan, P.; Storeng, R.; Scudiero, D.; Monks, A.; McMahon, J.; Vistica, D.; Warren, J.T.; Bokesch, H.; Kenney, S.; Boyd, M.R. New colorimetric cytotoxicity assay for anticancer-drug screening. *J. Natl. Cancer Inst.* **1990**, *82*, 1107–1112. [CrossRef]

23. DeLean, A.; Munson, P.J.; Rodbard, D. Simultaneous analysis of families of sigmoidal curves: Application to bioassay, radioligand assay, and physiological dose-response curves. *Am. J. Physiol.* **1978**, *235*, 97–102. [CrossRef]

24. Fomenko, I.; Durst, M.; Balaban, D. Robust regression for high throughput drug screening. *Comput. Methods Programs Biomed.* **2006**, *82*, 31–37. [CrossRef] [PubMed]

25. Gubler, H.; Schopfer, U.; Jacoby, E. Theoretical and experimental relationships between percent inhibition and IC50 data observed in high-throughput screening. *J. Biomol. Screen.* **2018**, *18*, 1–13. [CrossRef] [PubMed]

26. Evangelatov, A.; Skrobanska, R.; Mladenov, N.; Petkova, M.; Yordanov, G.; Pankov, R. Epirubicin loading in poly(butyl cyanoacrylate) nanoparticles manifests via altered intracellular localization and cellular response in cervical carcinoma (hela) cells. *Drug Deliv.* **2016**, *23*, 2235–2244.

27. Akter, M.; Sikder, M.T.; Rahman, M.M.; Ullah, A.K.M.A.; Hossain, K.F.B.; Banik, S.; Hosokawa, T.; Saito, T.; Kurasaki, M. A systematic review on silver nanoparticles-induced cytotoxicity: Physicochemical properties and perspectives. *J. Adv. Res.* **2018**, *9*, 1–16. [PubMed]

28. Zhang, H.Z.; Li, X.M.; Gao, F.P.; Liu, L.R.; Zhou, Z.M.; Zhang, Q.Q. Preparation of folate-modified pullulan acetate nanoparticles for tumor-targeted drug delivery. *Drug Deliv.* **2010**, *17*, 48–57. [PubMed]

29. Di-Wen, S.; Pan, G.Z.; Hao, L.; Zhang, J.; Xue, Q.Z.; Wang, P.; Yuan, Q.Z. Improved antitumor activity of epirubicin-loaded cxcr4-targeted polymeric nanoparticles in liver cancers. *Int. J. Pharm.* **2016**, *500*, 54–61. [PubMed]

30. Tariq, M.; Alam, M.A.; Singh, A.T.; Iqbal, Z.; Panda, A.K.; Talegaonkar, S. Biodegradable polymeric nanoparticles for oral delivery of epirubicin: In vitro, ex vivo, and in vivo investigations. *Colloid. Surf. B* **2015**, *128*, 448–456. [CrossRef] [PubMed]